THE ACOUSTIC AND INSTABILITY WAVES OF JETS CONFINED INSIDE AN ACOUSTICALLY LINED RECTANGULAR DUCT

FANG Q. HU

Department of Mathematics and Statistics
Old Dominion University
Norfolk, VA 23529

ABSTRACT

An analysis of linear wave modes associated with supersonic jets confined inside an acoustically lined rectangular duct is presented. Mathematical formulations are given for the vortex-sheet model and continuous mean flow model of the jet flow profiles. Detailed dispersion relations of these waves in a two-dimensional confined jet as well as an unconfined free jet are computed. Effects of the confining duct and the liners on the jet instability and acoustic waves are studied numerically. It is found that the effect of the liners is to attenuate waves that have supersonic phase velocities relative to the ambient flow. Numerical results also show that the growth rates of the instability waves could be reduced significantly by the use of liners. In addition, it is found that the upstream propagating neutral waves of an unconfined jet could become attenuated when the jet is confined.

---

1. INTRODUCTION

The exceedingly high level of jet noise presents a formidable barrier in developing future generation High Speed Civil Transport planes (see, e.g., Seiner [1]). In a proposed scheme of jet noise reduction, the exit jet of the engine is guided through a rectangular duct before discharged into the air. In the designing concept, the purpose of the duct is twofold. First, cold air could be sucked into the duct by the hot jet through the side inlets thus cool the jet streams and enhance the mixing. Second, the duct walls, installed with sound absorbing liners, could absorb a substantial part of the jet noise. It is important to understand and predict the generation, propagation and attenuation of jet noise inside a duct with sound absorbing liners. Furthermore, recent studies of supersonic jet noise generation mechanism have indicated that the growth of the instability waves of the jet is responsible for the dominant part of the jet noise (see, e.g., Tam and Burton [2]). In view of these studies, it is believed to be important to re-examine the jet instabilities with the confining lined walls.

Duct acoustics and wave attenuation by wall liners have been investigated extensively in the literature (see excellent reviews by Nayfeh, Kaiser and Telionis [3], Eversman [4] and references cited therein). Pridmore-Brown [5] first formulated the acoustic wave propagation problem in an attenuating duct with non-uniform mean flows. However, due to computational limitations, a majority of the early works have only considered duct flows with uniform mean velocity and temperature distributions. Later, with increased computing power, effects of the shear flow induced by the boundary layers at the duct walls were included in the acoustic wave attenuation calculations. In most studies, the shear flow of the boundary layer was approximated by a linear profile. It was found that the shear flow had a refraction effect on the wave propagations. It was also shown that solutions with a thin boundary layer converge to that of a uniform mean flow provided correct boundary conditions were used in the later (Eversman et al [6]). Most recently, Bies et al [7] presented a study that takes into account of the coupled effects of the acoustic waves inside the duct and those in the liners. However, historically, little attention has been paid to the instabilities of the shear flow inside the duct and its impact on sound generation.

Recently, the instability and acoustic waves associated with a planar mixing layer inside a rectangular duct have been studied by Tam and Hu [8]. Their main interest was in the instability of a confined mixing layer at supersonic velocities. They found that the instabilities of confined shear flows are quite different from that of their unconfined counterparts at high speeds. Systematic calculations of normal mode solutions showed

that new instability wave modes are induced by the coupled effect of the acoustic modes of the confining duct and the motion of the shear layer. It was also shown that at supersonic convective Mach numbers, acoustic waves that have supersonic phase velocities relative to both sides of the shear layer could be unstable (or amplified). The acoustic-mode instability of supersonic shear flows has also been found by Mack [9] for boundary layers and wakes, and for supersonic jets by Tam and Hu [10]. These studies have shown that at high supersonic speed, the acoustic-mode instability becomes the dominant flow instability.

In this paper, we carry out a detailed analysis of the linear wave modes associated with a given non-uniform mean flow inside a rectangular duct with finite wall impedance, including the acoustic waves and instability waves. The numerical results presented here are, however, limited to two-dimensional waves. Two models of the jet flow, a vortex-sheet model and a continuous mean flow model will be used. The mathematical formulation of the problems is given in Section 2. In Section 3 we present the numerical results and Section 4 contains the concluding remarks.

2. FORMULATIONS

2.1 MATHEMATICAL MODELS

We consider small amplitude waves associated with a given mean flow of a jet profile inside a rectangular duct (Figure 1). Here the mean velocities and densities of the jet core and the ambient stream will be denoted by u_j, ρ_j and u_a, ρ_a, respectively. The jet exit has a width of $2d$. The height of the duct is denoted by $2h$ and the width by B. The top and bottom walls of the duct are lined with acoustically treated materials with finite acoustic impedance. Two side walls are taken to be solid walls. For simplicity, we assume that the top and bottom walls are lined with the same materials. From linear stability considerations, the locally parallel flow assumption will be used through our study. To facilitate the numerical investigation, two models will be used in the present paper. In the first model, here referred to as the vortex-sheet model, the mean flow is piecewise uniform for the velocity and temperature. This profile models the flow near the nozzle exit. The advantage of the vortex-sheet model is that a closed form dispersion equation can be found. This allows for an extensive numerical study about the nature of all the wave modes. In the second model the mean flow is continuous. This permits more realistic flows and models the flow downstream of the nozzle exit.

2.2 GOVERNING EQUATIONS AND BOUNDARY CONDITIONS

We express each flow variable as a mean quantity plus a small perturbation as follows :

$$\begin{pmatrix} u(x,y,z,t) \\ v(x,y,z,t) \\ w(x,y,z,t) \\ p(x,y,z,t) \\ \rho(x,y,z,t) \end{pmatrix} = \begin{pmatrix} \bar{u}(y) \\ 0 \\ 0 \\ \bar{p} \\ \bar{\rho}(y) \end{pmatrix} + \begin{pmatrix} u'(x,y,z,t) \\ v'(x,y,z,t) \\ w'(x,y,z,t) \\ p'(x,y,z,t) \\ \rho'(x,y,z,t) \end{pmatrix}$$

In the above, the x coordinate is in the downstream direction, y is in the vertical direction and z is in the spanwise direction. u, v, w are the velocities in the x, y, z directions, respectively, p is the pressure and ρ is the density. An overbar indicates the mean quantity and prime indicates the perturbation. It is straight forward to find that the linearized governing equations for inviscid, non-heat-conducting fluids are :

$$\frac{\partial \rho'}{\partial t} + \bar{u}\frac{\partial \rho'}{\partial x} + \frac{d\bar{\rho}}{dy}v' + \bar{\rho}(\frac{\partial u'}{\partial x} + \frac{\partial v'}{\partial y} + \frac{\partial w'}{\partial z}) = 0 \qquad (2.1)$$

$$\frac{\partial u'}{\partial t} + \bar{u}\frac{\partial u'}{\partial x} + \frac{d\bar{u}}{dy}v' = -\frac{1}{\bar{\rho}}\frac{\partial p'}{\partial x} \qquad (2.2)$$

$$\frac{\partial v'}{\partial t} + \bar{u}\frac{\partial v'}{\partial x} = -\frac{1}{\bar{\rho}}\frac{\partial p'}{\partial y} \qquad (2.3)$$

$$\frac{\partial w'}{\partial t} + \bar{u}\frac{\partial w'}{\partial x} = -\frac{1}{\bar{\rho}}\frac{\partial p'}{\partial z} \qquad (2.4)$$

$$\frac{\partial p'}{\partial t} + \bar{u}\frac{\partial p'}{\partial x} + \gamma\bar{p}(\frac{\partial u'}{\partial x} + \frac{\partial v'}{\partial y} + \frac{\partial w'}{\partial z}) = 0 \qquad (2.5)$$

The temperature T is related to the pressure and density by the equation of state :

$$p = \rho R T \qquad (2.6)$$

To equations (2.1)-(2.5), we seek solutions of the form

$$\begin{pmatrix} u'(x,y,z,t) \\ v'(x,y,z,t) \\ w'(x,y,z,t) \\ p'(x,y,z,t) \\ \rho'(x,y,z,t) \end{pmatrix} = \begin{pmatrix} \hat{u}(y)\cos(2\pi m z/B) \\ \hat{v}(y)\cos(2\pi m z/B) \\ \hat{w}(y)\sin(2\pi m z/B) \\ \hat{p}(y)\cos(2\pi m z/B) \\ \hat{\rho}(y)\cos(2\pi m z/B) \end{pmatrix} e^{i(kx-\omega t)} \qquad (2.7)$$

By substituting (2.7) into equations (2.1)-(2.5) and proper boundary conditions, an eigenvalue problem is formed. In (2.7), the boundary conditions at two solid side walls, located at $z = \pm B/2$, have been satisfied automatically. At the acoustically treated top

3

and bottom walls, located at $y = \pm h$, the kinematic boundary condition is the continuity of particle displacement at the lined walls. For harmonic waves, it yields (Nayfeh et al [3])

$$\hat{v} = -\frac{(k\bar{u} - \omega)}{\omega Z}\hat{p} \tag{2.8}$$

where Z is the wall impedance ($Z = \frac{p_{wall}}{v_{wall}}$).

In (2.7), m is a modal number indicating wave reflections in the z direction. When $m = 0$, the waves are two-dimensional. The mathematical formulation of the eigenvalue problems for the vortex-sheet model and the continuous mean flow profile model is given below.

2.3 VORTEX-SHEET MODEL

For the vortex-sheet model the jet boundaries are represented by infinitely thin vortex sheets. Thus the mean flow is piecewise uniform and a closed form dispersion equation can be found. In addition, due to the symmetry of the mean flow, it is convenient to consider symmetric ($\frac{d\hat{p}(0)}{dy} = 0$) and antisymmetric ($\hat{p}(0) = 0$) wave modes separately. As a result only the flow in the upper half of the duct needs to be considered. By satisfying the boundary conditions at the wall and the jet interface, the dispersion equation which implicitly relates ω and k is found as follows :

Symmetric Modes :

$$\frac{\lambda_j \tan(\lambda_j d)}{\rho_j(\omega - ku_j)^2} - \frac{\lambda_a}{\rho_a(\omega - ku_a)^2}\frac{\rho_a(\omega - ku_a)^2 \cos[\lambda_a(h-d)] - i\omega\lambda_a Z \sin[\lambda_a(h-d)]}{\rho_a(\omega - ku_a)^2 \sin[\lambda_a(h-d)] + i\omega\lambda_a Z \cos[\lambda_a(h-d)]} = 0 \tag{2.9a}$$

Antisymmetric Modes :

$$\frac{\lambda_j \cot(\lambda_j d)}{\rho_j(\omega - ku_j)^2} + \frac{\lambda_a}{\rho_a(\omega - ku_a)^2}\frac{\rho_a(\omega - ku_a)^2 \cos[\lambda_a(h-d)] - i\omega\lambda_a Z \sin[\lambda_a(h-d)]}{\rho_a(\omega - ku_a)^2 \sin[\lambda_a(h-d)] + i\omega\lambda_a Z \cos[\lambda_a(h-d)]} = 0 \tag{2.9b}$$

where

$$\lambda_a = \sqrt{\left(\frac{\omega - ku_a}{c_a}\right)^2 - k^2 - \left(\frac{2m\pi}{B}\right)^2}$$

$$\lambda_j = \sqrt{\left(\frac{\omega - ku_j}{c_j}\right)^2 - k^2 - \left(\frac{2m\pi}{B}\right)^2}$$

and the speeds of sound are given by $c_{a,j} = \sqrt{\frac{\gamma p}{\rho_{a,j}}}$.

4

Here it is interesting to note two special cases of the dispersion equations given above, i.e., when the mean flow is uniform and when the duct walls are solid boundaries.

Uniform mean flow

For a uniform flow profile inside the duct, we have $u_a = u_j$, $\rho_a = \rho_j$ and $d = h$. The dispersion relation equations (2.9a) and (2.9b) then become

$$\tan(\lambda_j d) - \frac{\rho_j(\omega - ku_j)^2}{i\omega\lambda_j Z} = 0$$

for symmetric modes and

$$\cot(\lambda_j d) + \frac{\rho_j(\omega - ku_j)^2}{i\omega\lambda_j Z} = 0$$

for antisymmetric modes, respectively. The above two equations are the same as those obtained in the literature for uniform mean flows (Nayfeh et al [3]).

Solid walls

For solid walls, $Z \to \infty$. In this case, The dispersion relation equation (2.9a) and (2.9b) reduces to

$$\frac{\lambda_j \tan(\lambda_j d)}{\rho_j(\omega - ku_j)^2} + \frac{\lambda_a \tan[\lambda_a(h-d)]}{\rho_a(\omega - ku_a)^2} = 0$$

for symmetric modes (Tam and Hu [8]) and

$$\frac{\lambda_j \cot(\lambda_j d)}{\rho_j(\omega - ku_j)^2} - \frac{\lambda_a \tan[\lambda_a(h-d)]}{\rho_a(\omega - ku_a)^2} = 0$$

for antisymmetric modes, respectively.

2.4 CONTINUOUS MEAN FLOW MODEL

For continuous mean flow profiles, upon substituting (2.7) into (2.1) - (2.5), the linearized governing equations can be reduced to a single equation for the pressure perturbation as given below :

$$\frac{d^2\hat{p}}{dy^2} + \left(\frac{2k}{\omega - k\bar{u}} \frac{d\bar{u}}{dy} - \frac{1}{\bar{\rho}} \frac{d\bar{\rho}}{dy} \right) \frac{d\hat{p}}{dy} + \left[\left(\frac{\omega - k\bar{u}}{\bar{c}} \right)^2 - k^2 - \left(\frac{2m\pi}{B} \right)^2 \right] \hat{p} = 0 \qquad (2.10)$$

where $\bar{c}$ is the speed of sound.

The boundary conditions for $\hat{p}$ are, at $y = h$,

$$\hat{p} + \frac{i\omega Z}{\bar{\rho}_a(\omega - k\bar{u}_a)^2} \frac{d\hat{p}}{dy} = 0 \qquad (2.11)$$

5

and, at $y = 0$,

$$\frac{d\hat{p}}{dy} = 0 \quad \text{(symmetric modes)} \tag{2.12a}$$

or

$$\hat{p} = 0 \quad \text{(antisymmetric modes)} \tag{2.12b}$$

Equation (2.10) and the boundary conditions (2.11), (2.12) form an eigenvalue problem. The problem will be solved numerically by integrating from the center line $y = 0$ to the upper boundary $y = h$ and employing a shooting method using the results of the vortex-sheet model as the starting solutions.

3. NUMERICAL RESULTS

For numerical results shown below, the Mach numbers of the jet and ambient flow are $M_j = 2.0$ and $M_a = 0.2$ respectively. The speeds of sound ratio $c_a/c_j = 0.5$. All the results shown are with respect to two-dimensional symmetric wave modes. Results of antisymmetric modes are similar and not shown here.

3.1 RESULTS OF THE VORTEX-SHEET MODEL

Our main interest is to determine the normal modes associated with a two-dimensional supersonic jet confined inside a duct and study the effects of the confining lined walls on these wave modes. For the purpose of making comparisons, the dispersion relations of an *unconfined* jet will be discussed briefly.

3.1.1 *Unconfined jets*

The normal modes of a free circular jet has been studied extensively by Tam and Hu [10]. Here some properties of a two-dimensional free jet will be examined briefly.

For a two-dimensional free jet, the dispersion equation relating the frequency ω and wavenumber k is given by :

$$\frac{i\lambda_a \cos(\lambda_j d)}{\rho_a(\omega - ku_a)^2} + \frac{\lambda_j \sin(\lambda_j d)}{\rho_j(\omega - ku_j)^2} = 0 \tag{3.1a}$$

for the symmetric modes and

$$\frac{i\lambda_a \sin(\lambda_j d)}{\rho_a(\omega - ku_a)^2} - \frac{\lambda_j \cos(\lambda_j d)}{\rho_j(\omega - ku_j)^2} = 0 \tag{3.1b}$$

6

for the antisymmetric modes (Gill [11]). The dispersion relation of the symmetric modes has been computed here and is shown in Figure 2, (k_r and k_i are the real and imaginary parts of the wavenumber k). Our numerical studies of the dispersion equation (3.1a) indicate that the present 'top hat' jet profile possesses instability waves as well as neutrally stable acoustics waves. Furthermore, since the convective Mach number (here defined as $M_c = (u_j - u_a)/(c_j + c_a)$) is greater than one in the present case, a family of supersonic instability waves is also present in addition to the Kelvin-Helmholtz instability wave. This family of unstable modes have supersonic phase velocities relative to both the jet and the ambient streams. The properties of these supersonic instability waves were more fully discussed in Tam and Hu [10].

In addition to the unstable wave modes, namely the K-H wave and the supersonic instability waves, there are also two families of neutrally stable waves associated with the free jet. Here we should refer to these two families as the family C and family D acoustic waves. For convenience of discussion, we should also divide the $k_r - \omega$ plane into five regions by the sonic lines as indicated in the figure. Two aspects of the neutral acoustic waves are worth pointing out. First, we note that the neutral waves are found only in region I, above the sonic line $\omega/k_r = u_a + c_a$ or in region II, below the sonic line $\omega/k_r = u_a - c_a$. That is, the phase velocity, $C_{ph} = \omega/k$, of the neutral wave is always subsonic relative to the ambient, i.e. $|C_{ph} - u_a| \le c_a$. For class C waves we get $0 \le C_{ph} \le u_a + c_a$ and for class D waves we get $u_a - c_a \le C_{ph} \le 0$. In other words, for the free jet, the neutral waves attached the jet are necessarily decaying away from the jet. Second, it has been found that part of the class D waves represent upstream waves with a phase velocity close to $u_a - c_a$ as indicated in Figure 2 (see also Tam and Hu [10]). This means that it is possible to have upstream propagating neutral waves attached to the jet even though the jet mean velocity is supersonic. This point will be re-examined more closely later.

3.1.2 *Confined jets*

We now turn to the effects of the duct walls and compute the normal modes associated with a confined jet. We first deal with the case when the duct walls are solid boundaries. The case when the duct walls are lined will be dealt with in Section 3.1.3. For solid walls, we let $Z \to \infty$ in (2.9). With the vortex sheet model, the frequency and wavenumber of the wave modes are then the roots or zeroes of the dispersion equation (2.9a) or (2.9b). In the present work, we are interested in the spatially attenuating or growing waves. Thus ω will be a real number. However, for systems that have spatial instabilities, it is not sufficient to just set the frequency ω to be a real number and look for the zeroes of the

dispersion equations in the complex k-plane. One must distinguish the downstream and upstream propagating waves. Without the proper distinction, a downstream-propagating growing wave may be erroneously considered as an upstream-propagating attenuating wave and vice versa. For this reason, the criterion developed by Briggs [12] and also used by Tam and Hu [8] will be followed here. In this procedure, the frequency ω is first given a complex number whose real part is the frequency of interest and imaginary part is some large number. Then the corresponding zeroes of the dispersion equation are found in the complex k-plane. A ω-contour deformation process is applied in which the real part of the ω is kept constant while the imaginary part of ω is gradually reduced to zero. In this process, the corresponding zeroes of the dispersion equation in the k-plane is traced as the imaginary part of the ω is being reduced. In Briggs' criterion, the zeroes originated from the upper half k-plane then represent the downstream propagating waves and the zeroes from the lower half k-plane represent the upperstream propagating waves.

To illustrate the above process, the traces of the zeroes in the k-plane as the imaginary part of ω is being reduced are plotted in Figure 3 for the case of real$(\omega d/u_j) = 3$. In this way, the propagation direction of wave mode associated with each zero in the k-plane is correctly identified. Those zeroes that move across the real k-axis will represent instability waves. Those zeroes that remain in the upper or lower half k-plane then represent decaying or attenuated waves. Moreover, zeroes that lie on the real k-axis in Figure 3 represent the neutrally stable acoustic waves.

The above procedure has been applied systematically as the real part of ω changes. The dispersion relations so obtained are given in Figure 4. (Similar procedure has been used in the free jet calculations given in the previous section). Here for convenience of discussion, wave modes have been classified into two families of unstable waves, the A and B modes, and two families of neutrally stable acoustic waves, the C and D waves. However, a detailed description of the characteristics of each family of the waves will not given here. They are quite similar to the four families previously found in a planar mixing layer (Tam and Hu [8]).

We now compare the dispersion relation of the confined jet given in Figure 4 with that of an unconfined free jet shown in Figure 2. We first note that, due to the confinement, the neutral waves can have phase speed supersonic to the ambient flow. The dispersion relation curves for family C and family D neutral waves now extend across the sonic line $C_{ph} = u_a \pm c_a$ continuously.

Furthermore, a close inspection of Figure 4, the dispersion relation diagram, shows

that the family D waves now all have a positive group velocities. To study the upstream waves, in Figure 5, the real and imaginary parts of k as a function of ω are plotted for the first three zeroes that originate from the lower half k-plane in the contour deformation process. It is seen that although these wave numbers have negative imaginary parts, they are actually attenuating waves as they are upstream propagating waves. Careful numerical computations show that for $\omega d/u_j < 4$, no zero reaches the real k-axis from below. In other words, low frequency upstream propagating waves of the free jet are attenuated due to the presence of the confining walls.

Since the upstream propagating waves of the unconfined jet have phase velocities close to $u_a - c_a$ in the unconfined jets (see Figure 2), we can now calculate the group velocity, $\partial \omega/\partial k$, for neutral waves along the sonic line $C_{ph} = u_a - c_a$. By letting $\omega/k = u_a - c_a$, the derivative $\partial \omega/\partial k$ can be obtained analytically from the dispersion equations given by (2.9a) and (2.9b). The expression for $\partial \omega/\partial k$ is not given here for brevity. To have neutral waves that travel upstream, it is necessary that $\partial \omega/\partial k < 0$. It is found that, for both the symmetric and antisymmetric modes, this requires that

$$\frac{h-d}{d} > \frac{c_a u_j(u_j + c_a - u_a) - c_j^2 c_a}{2(c_a - u_a)(u_j + c_a - u_a)^2}$$

or in non-dimensional parameters,

$$\frac{h-d}{d} > \frac{M_j[M_j + (1 - M_a)\dfrac{c_a}{c_j}] - 1}{2(1 - M_a)[M_j + (1 - M_a)\dfrac{c_a}{c_j}]^2} \tag{3.2}$$

Figure 6 plots the boundary curves in the space of M_j v.s. d/h for different ambient Mach numbers. Asymptotically, for hot jets and low Mach number in the ambient, the upstream waves are attenuated when $d/h > 2/3$. For cold jets, this condition is $d/h > 3/4$.

3.1.3 *Effects of wall liners*

We now study the effects of the finite wall impedance of the liners on the acoustic and the instability waves discussed in the previous section. A point-reacting wall impedance model will be used in the present study. In this model, the impedance of the wall is given by

$$Z = \rho_a c_a \left[R + i \cot(\frac{\omega \ell}{c_a}) \right] \tag{3.4}$$

where ρ_a, c_a are the density and speed of sound of the ambient fluid, ℓ is the thickness of the liner cavity and R is the resistance (non-dimensional) of the wall facing the flow. In all the results reported below, we have used $\ell = 0.05h$ and varied R.

9

Numerical calculations show that the liner effect varies for waves in different regions in the dispersion diagram. For instance, for the acoustic waves in regions I and V, the phase velocity is subsonic relative to the ambient flow but supersonic relative to the jet. These waves are trapped inside the jet and their eigenfunctions decay away from the jet. The effect of the liner is thus minimal. On the other hand, for acoustic waves in regions II, III and V, the phase velocity is supersonic relative to the ambient flow. Their eigenfunctions show a larger pressure perturbation at the wall. Thus a larger influence of the liner was found on the wave modes in these regions. This is clearly shown in Figure 7 where eigenfunctions of selected wave modes for solid and lined walls are plotted. Also plotted are the eigenfunctions of A and B instability wave modes. For family A waves, the eigenfunction has a peak at the jet boundary, $y = 0.75h$, and decays towards the wall. The effects of the lined walls thus are not significant. For the B modes, however, the eigenfunction decays slowly towards the wall. For this family of waves, a larger effect of the lined walls was shown.

In Figure 8 we show the effects of the acoustic liner on the growth rates of the instability waves. Plotted are the spatial growth rates of the first three family A waves for wall resistance $R = 1, 2, 5$ respectively. Clearly the growth rates are reduced when finite impedance walls are used. However we also point out that the attenuation effects are not significant for second and third modes, namely A_2 and A_3 modes.

In Figure 9 the effects of the liners on the acoustic modes are shown. Plotted are the imaginary parts of the complex wave number as functions of $1/R$. It is seen that with lined walls, the family D waves are attenuated but the family C waves are actually destablized. Further investigation have indicated that this destablization is a direct result of the merging of the C and unstable B waves when the impedance Z becomes a complex number. Again it is clear from Figure 9 that the degree of influence on the liners on the acoustic waves depends largely on the phase velocity of the waves and thus the region in the dispersion diagram. The least affected are the waves in regions I and V in which the phase velocity of the wave is subsonic relative to the ambient flow.

3.2 RESULTS OF THE CONTINUOUS MEAN FLOW MODEL

For the continuous mean flow model, we have used a hyperbolic tangent for the mean velocity profile, namely,

$$\bar{u}(y) = \frac{1}{2} \left\{ \bar{u}_a + \bar{u}_j - (\bar{u}_a - \bar{u}_j) \tanh[2(|y| - d)/\delta_\omega] \right\}$$

and obtained the mean temperature profile from the Crocco's relations (Hu [13]). Here δ_ω represents the vorticity thickness of the shear layer. Our study with the finite thickness mean velocity profile will be emphasized on the liner effects on the instability waves. In particular, only the family A instability waves will be examined here since they have larger growth rates than the family B modes.

In Figure 10, the growth rate $(-k_i d)$ as a function of the vorticity thickness is given for the most amplified A_1 and A_2 modes. Calculations were made for both the solid and lined walls. In general, as the thickness of the jet shear layer increases, the growth rate of the instability waves decreases. However it is clear from the results shown that the liner becomes more effective in reducing the growth rates of the instability waves when the finite thickness effects are considered. In Figure 11 we show the variation of the eigenfunctions as the thickness of the jet shear layer increases. It is seen that as the thickness increases, the relative peak of the eigenfunction at the jet boundary is reduced. As a result the influence of the wall boundary condition increases. Based on the results shown, for a realistic jet flow with a finite vorticity thickness, say $\delta_\omega > 0.05d$, the acoustic liner can reduce the growth rate of the instability waves quite significantly.

4. CONCLUDING REMARKS

A detailed analysis of the linear wave modes associated with a jet confined inside acoustically lined duct walls has been carried out. The dispersion relations of the acoustic and instability waves have been computed and given for the two-dimensional modes. In particular, the effects of the confining walls and the liners on the linear waves of the jet have been studied. It is found that the effect of the liners is to attenuate waves that have supersonic phase velocities relative to the ambient flow. The attenuation, however, is less effective for the waves that have a subsonic phase velocity relative to the ambient flow. In addition, it is found that due to the presence of the confining walls, the upstream propagating waves associated with a free supersonic jet could become attenuated under given conditions. Furthermore, it is shown that, with a finite shear layer thickness, the acoustic liners have a quite significant effect in reducing the growth rates of the instability waves of the jet.

In view of recent studies on supersonic jet noise generation mechanism [2], the growth of the instability waves of the jet plays a central role in the noise generation. The results of the present study indicate that growth rates of the instability waves can be reduced greatly by employing lined walls. It is then reasonable to expect that this reduction in the

growth rate of the instability waves may not only result in a change in the hydrodynamics (spreading rate, turbulent structures) but also result in a change in the noise generation of the jet. Moreover, in recent studies of jet screech tone noises, it has been suggested that the upperstream propagating waves of the free jet is an essential part of the feed-back mechanism (Tam and Norum [14]). The present study, however, shows that these upstream propagating waves could become attenuated due to the confinement of the jet. It will be interesting and challenging to further examine and explore the direct consequences of these wave propagation properties on the noise generation. This, however, is beyond the scope of this study.

ACKNOWLEDGMENTS

REFERENCES

1. Seiner, J.M. 1992 In *Studies in Turbulences*, 297-323, Springer-Verlag. Fluid dynamics and noise emission associated with supersonic jets.

2. Tam, C.K.W. & Burton, D.E. 1984 *J. Fluid Mech.* **138**, 273-295. Sound generated by instability waves of supersonic flows. Part 2. Axisymmetric jets.

3. Nayfeh, A. H, Kaiser, J.E. and Telionis, D.P 1975 *AIAA*, **13**, No.2, 130-153. Acoustics of aircraft engine-duct systems.

4. Eversman, W. 1991 *aeroacoustics of Flight Vehicles : Theory and Practice*, NASA RP 1258, Vol.2, 101-163. Theoretical Models for duct acoustic propagation and radiation.

5. Pridmore-Brown, D.C. 1958 *J. Fluid Mech.* **4**, 393-406. Sound propagation in a fluid flowing through an attenuating duct.

6. Eversman, W. and Beckemeyer, H.E. 1972 *The Journal of the Acoustic Society of America*, **52**, No.1, Pt. 2, 216-220. Transmission of sound in ducts with thin shear layers-convergence to the uniform flow case.

7. Bies, D.A., Hansen, C.H. and Bridges, G.E. 1991 *J. Sound and Vib.*, **146**, No.1, 47-80. Sound attenuation in rectangular and circular cross-section ducts with flow and bulk-reacting liners.

8. Tam, C.K.W & Hu, F.Q. 1989 *J. Fluid Mech.* **203**, 51-76. The instability and acoustic wave modes of supersonic mixing layers inside a rectangular channel.

9. Mack, L.M. 1990 *Theoretical and Computational Fluid Dynamics* **2**, 97-123. On the inviscid acoustic-mode instability of supersonic shear flows. Part 1 : Two-dimensional waves.

10. Tam, C.K.W. & Hu, F.Q. 1989 *J. Fluid Mech.* **201**, 447-483. On the three families of instability waves of high-speed jets.

11. Gill, A.E. 1965 *Phys. Fluids* **8**, 1428-1430. Instability of top-hat jets and wakes in compressible fluids.

12. Briggs, R.J. 1964 *Electron-stream interaction with plasmas*. MIT Press.

13. Hu, F.Q. 1993 *Phy. Fluids* **5** (6), 1420-1426. A numerical study of wave propagation in a confined mixing layer by eigenfunction expansions.

14. Tam, C.K.W. & Norum, T.D. 1992 *AIAA J.* **30**, No. 2, 304-312. Impingement tones of large aspect ratio supersonic rectangular jets.
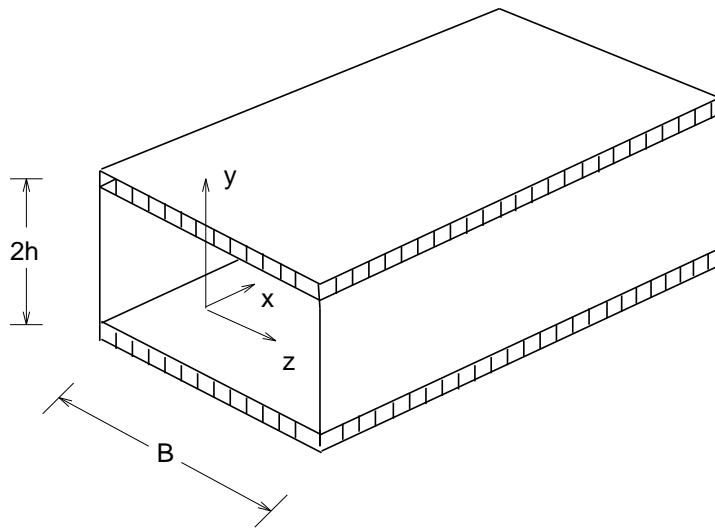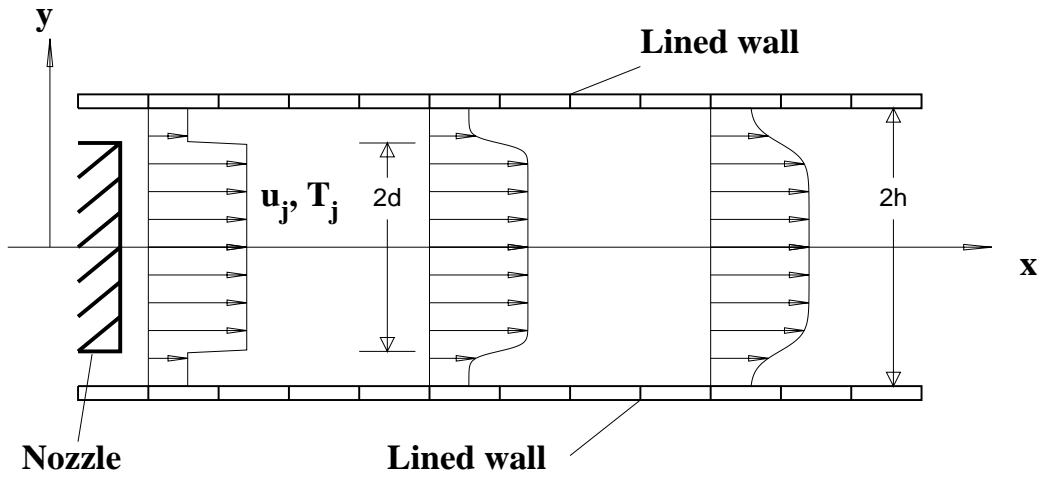
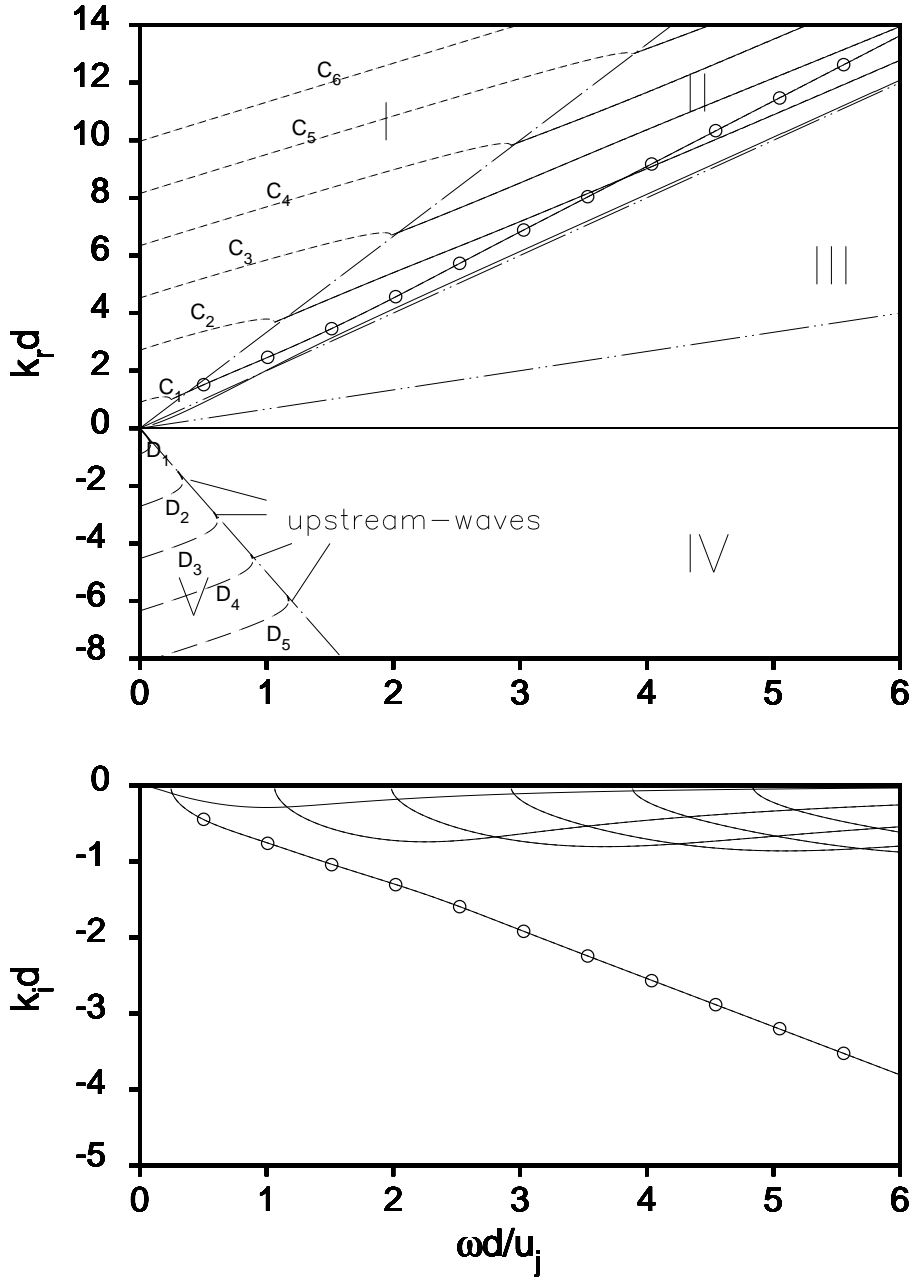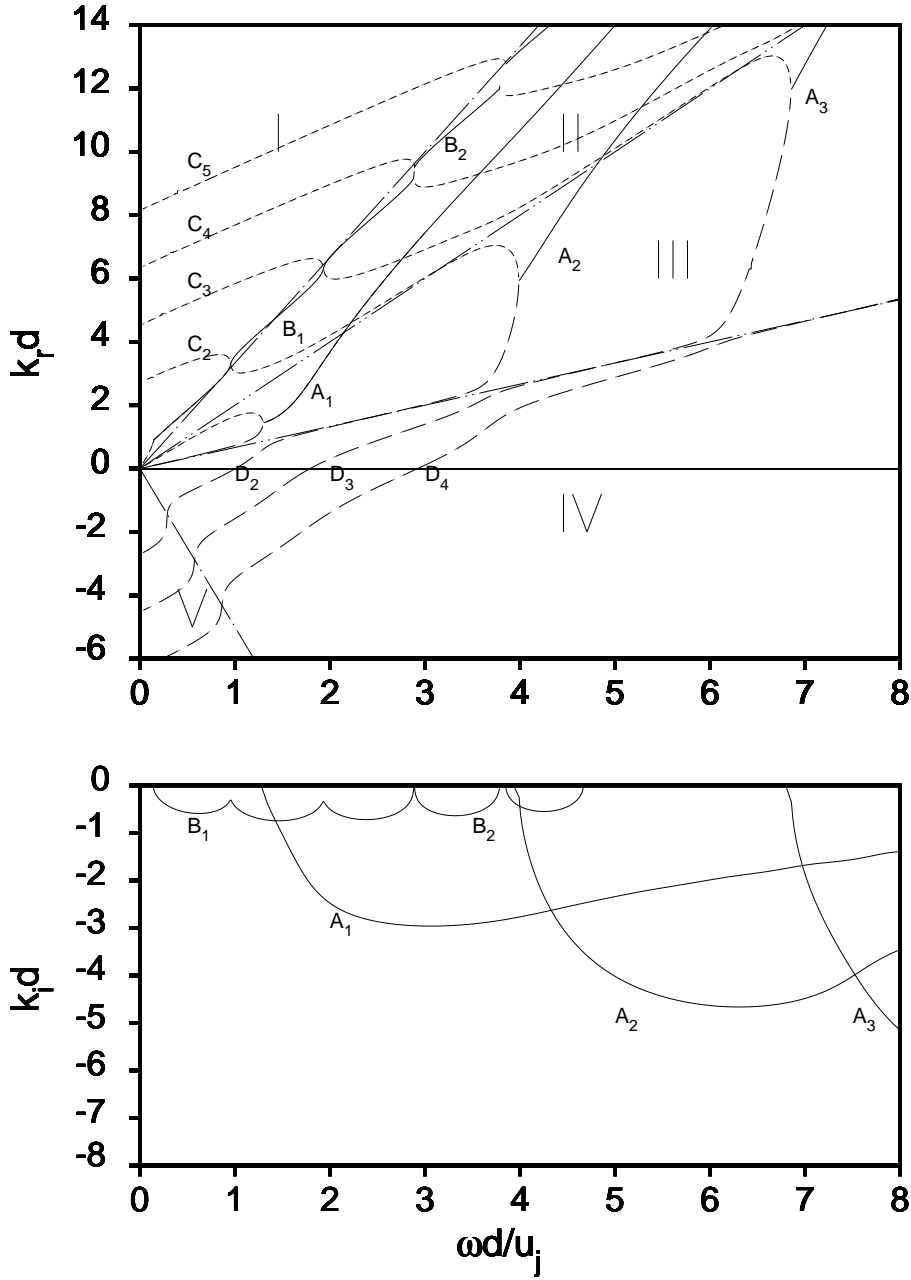Figure 1. Schematic of a confined jet with lined walls.

Figure 2. Dispersion relation of an unconfined jet. Shown are the symmetric modes. $M_j = 2.0, M_a = 0.2$, $c_a/c_j = 0.5$. —o— Kelvin-Helmholtz mode, ——— supersonic instability modes, - - - - - family C modes, — — — family D modes. — · — · — sonic lines $\omega/k_r = u_a \pm c_a$, — · · — · · — sonic lines $\omega/k_r = u_j \pm c_j$.

Figure 3. Trajectories of zeroes of the dispersion equation in the complex k plane as $\omega d/u_j$ is varied from 3+5i to 3. Shown are the symmetric modes with solid walls. $M_j = 2.0$, $M_a = 0.2$, $c_a/c_j = 0.5$, $d/h = 0.75$.

Figure 4. Dispersion relation of an confined jet. Shown are the symmetric modes. $M_j = 2.0$, $M_a = 0.2$, $c_a/c_j = 0.5$, $d/h = 0.75$, solid walls at $y = \pm h$. ————— unstable modes, - - - - - - family C modes, — — — — family D modes. — · — · — sonic lines $\omega/k_r = u_a \pm c_a$, — · · — · · — sonic lines $\omega/k_r = u_j \pm c_j$.

18
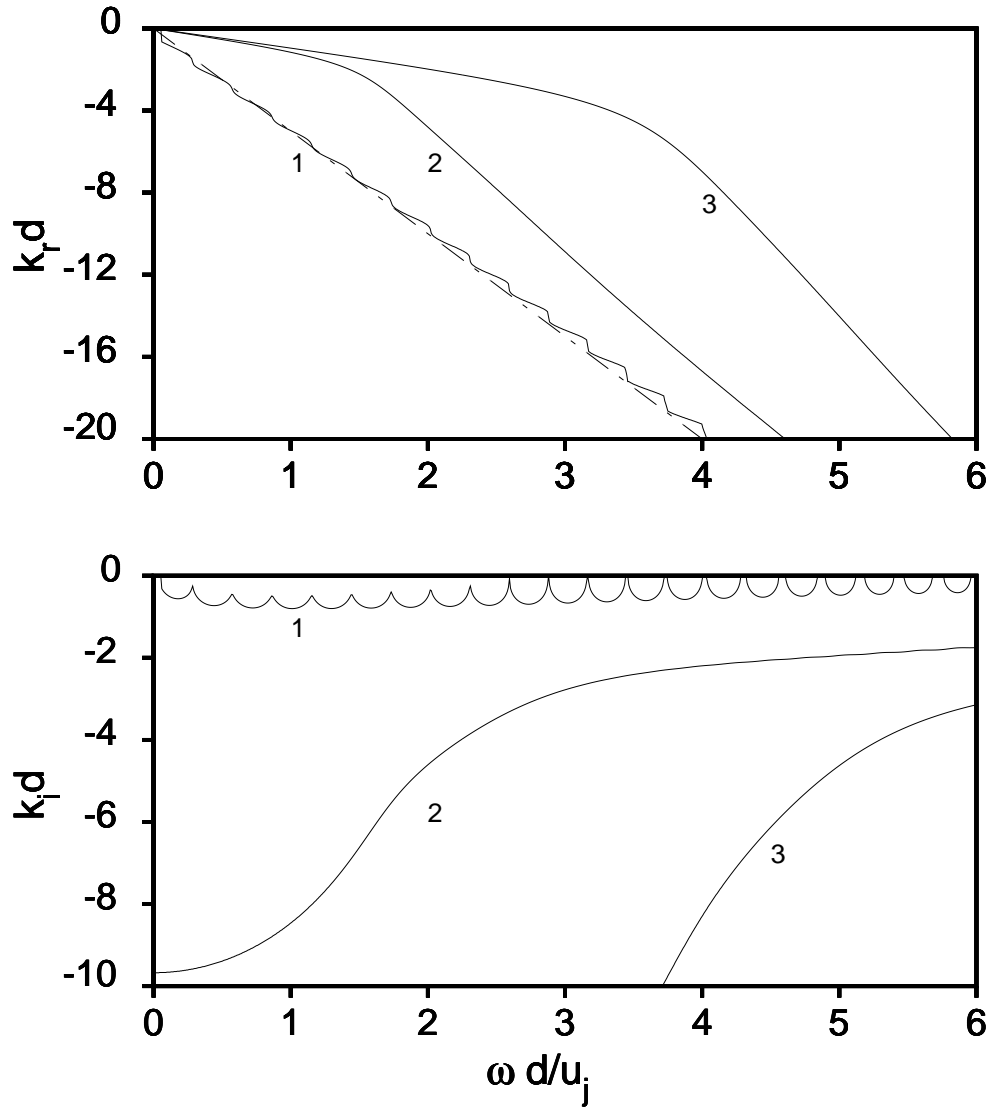
Figure 5. Dispersion relation of the upstream propagating waves. $M_j = 2.0$, $M_a = 0.2$, $c_a/c_j = 0.5$, $d/h = 0.75$, solid walls.
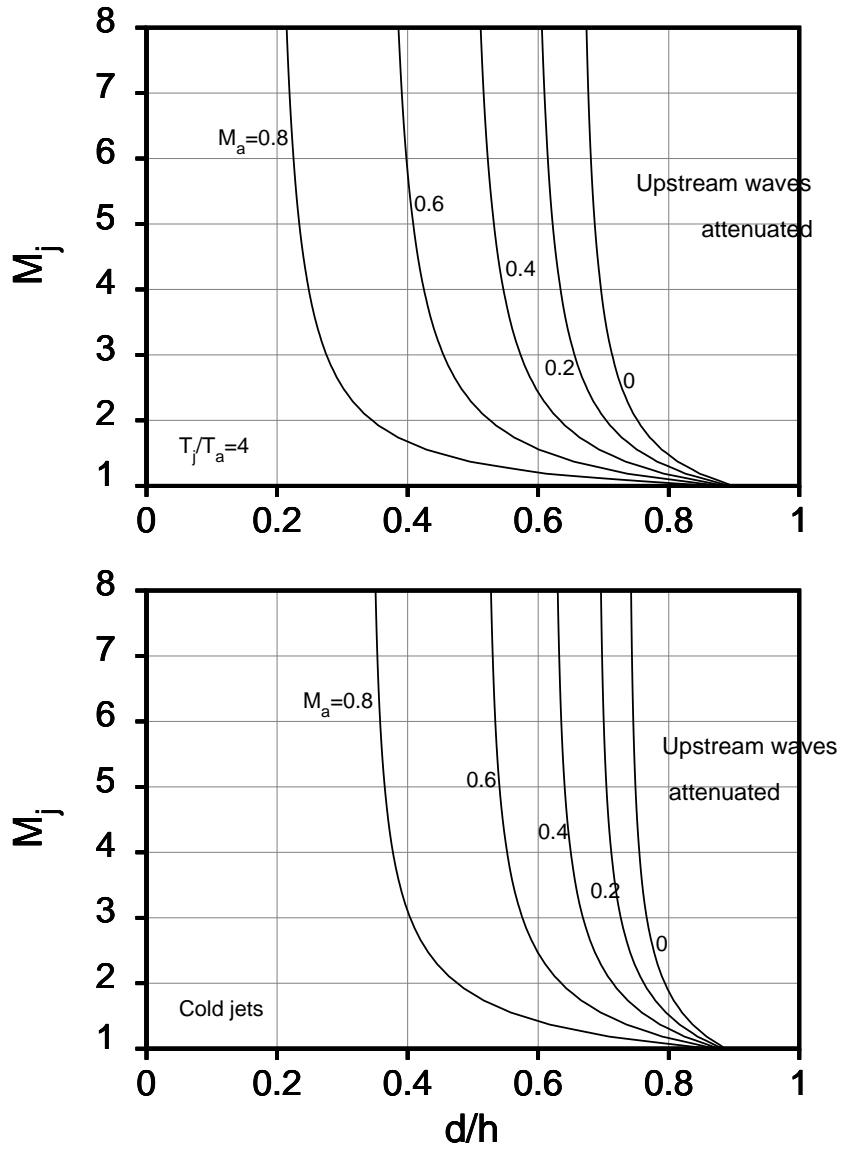
Figure 6. Boundaries for attenuation of the upstream propagating waves.
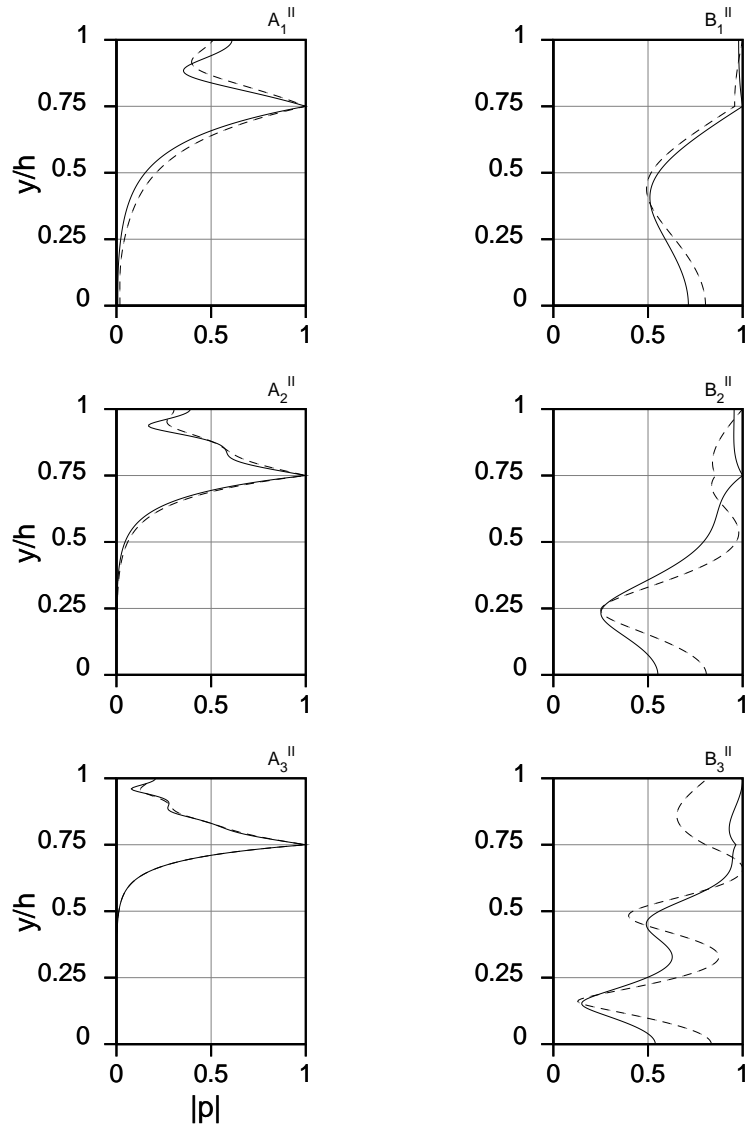
Figure 7(a)
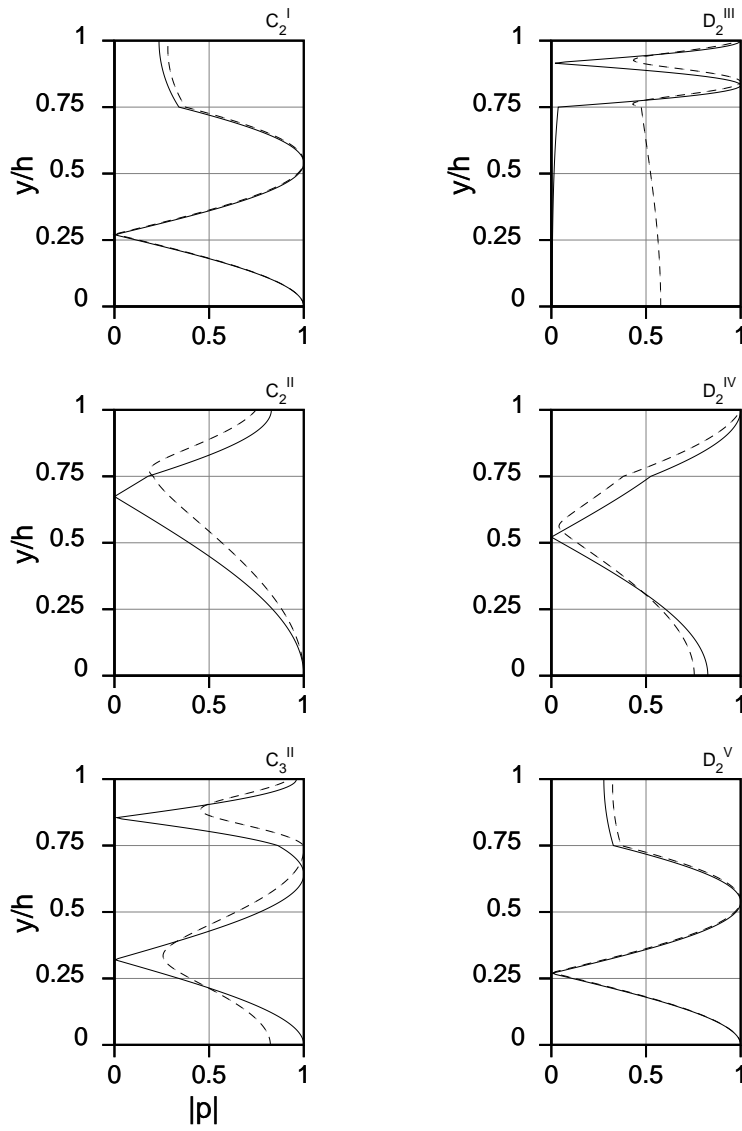
Figure 7(b)

Figure 7. Eigenfunctions for selected waves modes. ——— solid walls, - - - - - lined walls with $R = 2$. Superscripts indicate the regions of the wave mode in Figure 4. Symmetric modes, $M_j = 2.0$, $M_a = 0.2$, $c_a/c_j = 0.5$, $d/h = 0.75$.
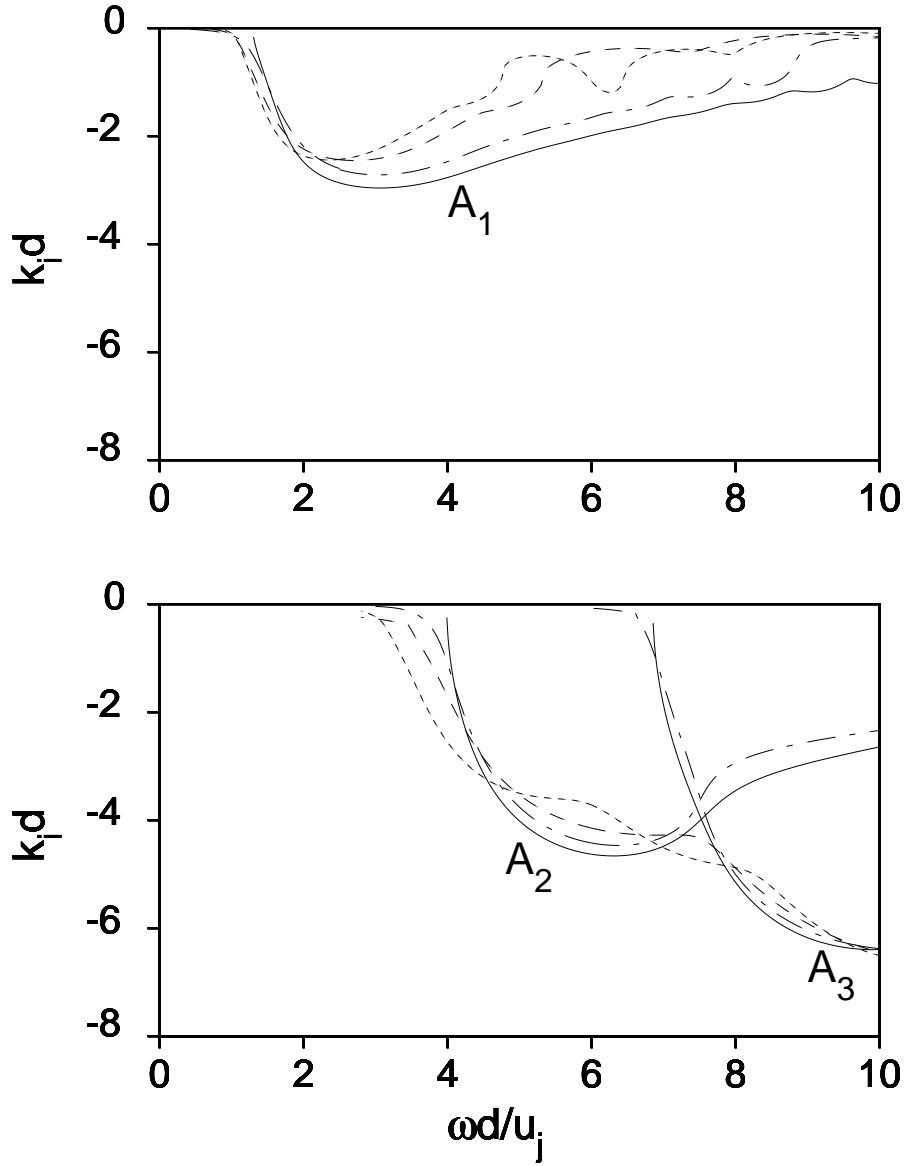
Figure 8. Growth rates of A_1, A_2 and A_3 modes. ———— solid walls, — · — · — R=5, — — — R=2, - - - - - R=1. Symmetric modes, $M_j = 2.0$, $M_a = 0.2$, $c_a/c_j = 0.5$, $d/h = 0.75$.
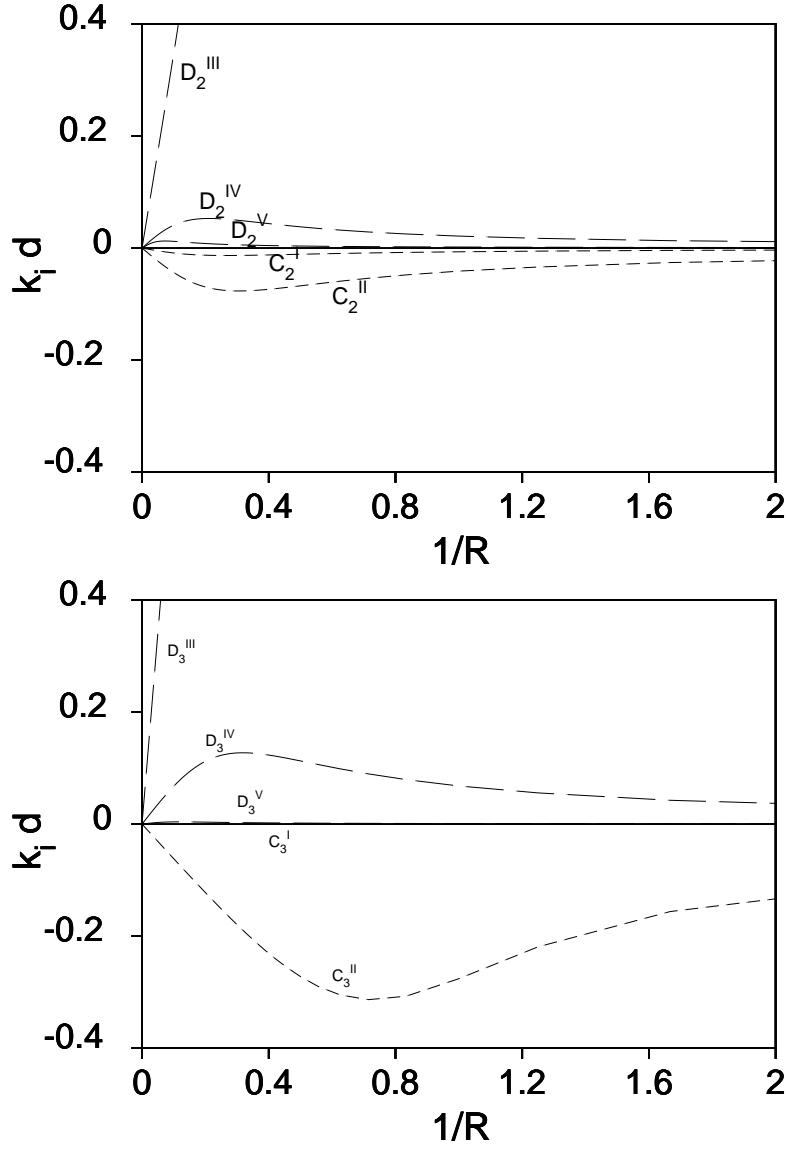
Figure 9. k_i as a function of $1/R$ for the C and D wave modes. Superscripts indicate the regions of the wave mode in Figure 4. Symmetric modes, $M_j = 2.0$, $M_a = 0.2$, $c_a/c_j = 0.5$, $d/h = 0.75$.
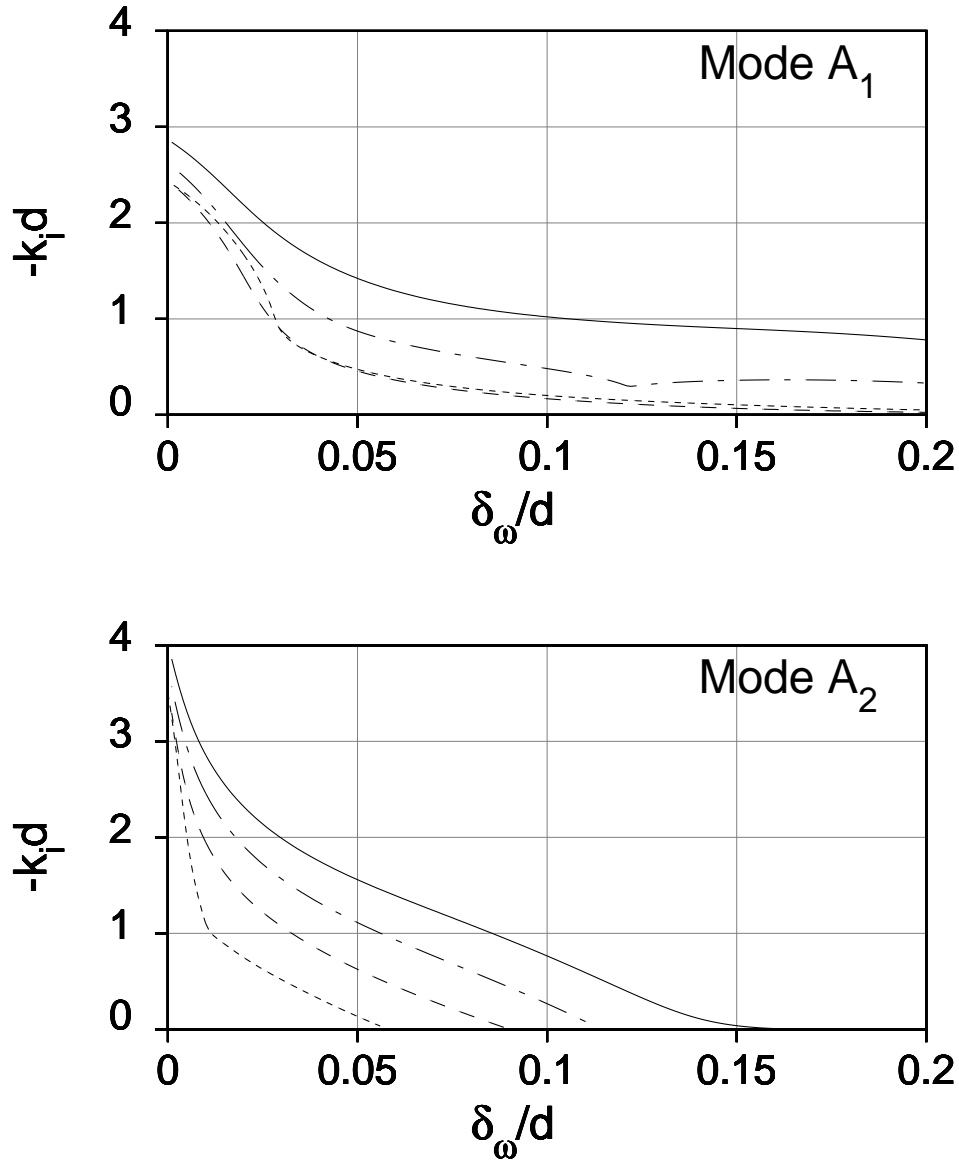
Figure 10. Growth rates of the most unstable A_1 and A_2 modes as functions of jet mixing layer thickness. ———— solid walls, — · — · — R=5, — — — R=2, - - - - - R=1. Symmetric modes, $M_j = 2.0$, $M_a = 0.2$, $c_a/c_j = 0.5$, $d/h = 0.75$.
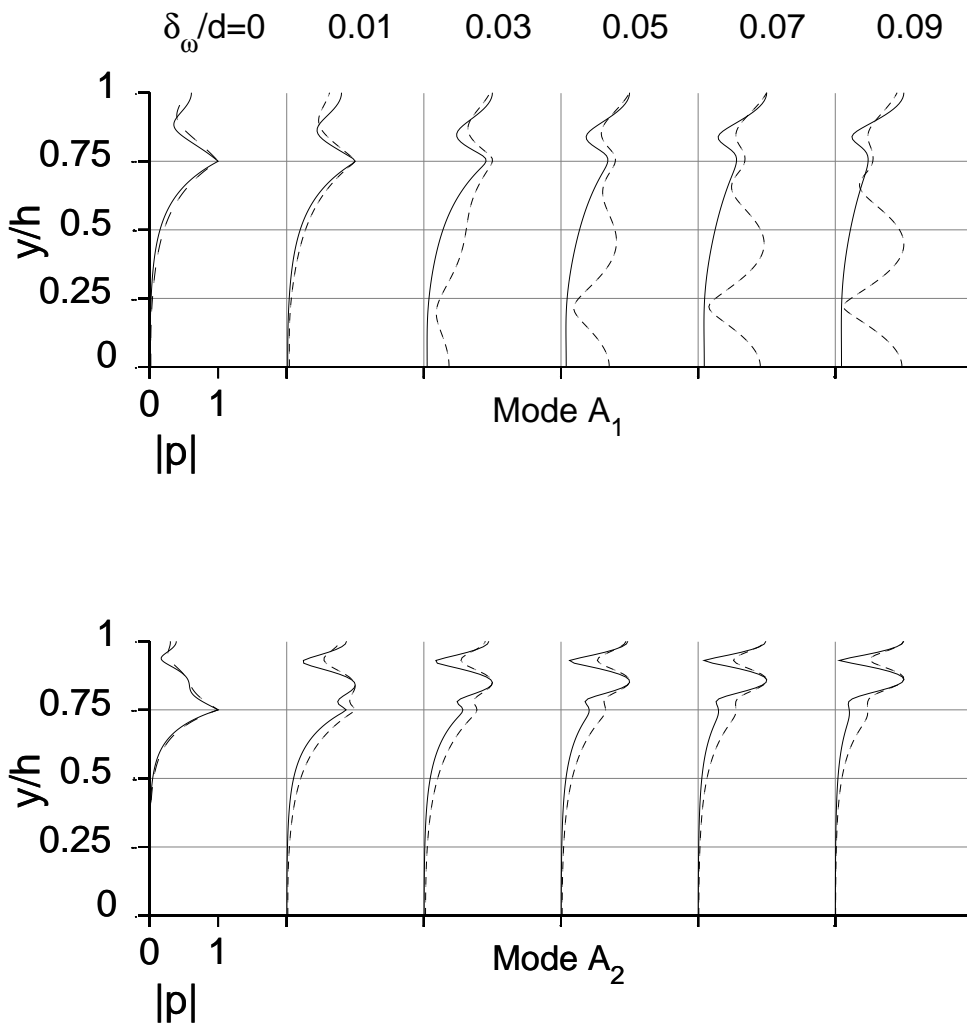
Figure 11. Eigenfunctions of the most unstable A_1 and A_2 modes as thickness varies. ———— solid wall, - - - - - R=2.